

Supplementary Information

Bone-on-leaf-chip for the study of lung cancer bone metastasis

Qi Liu^{ab}, Di Suo^{ab}, Renxian Wang^e, Shuai Zhao^{ab}, Mao Mao^c, Wei-Ning Lee^e, Yuhe Yang^{*ab} and Xin Zhao^{*abd}

^a. Department of Applied Biology and Chemical Technology, the Hong Kong Polytechnic University, Hung Hom, Kowloon, Hong Kong SAR, China.

^b. The Hong Kong Polytechnic University Shenzhen Research Institute, Shenzhen, China.

^c. State Key Laboratory for Manufacturing Systems Engineering, Xi'an Jiaotong University, Xi'an, China.

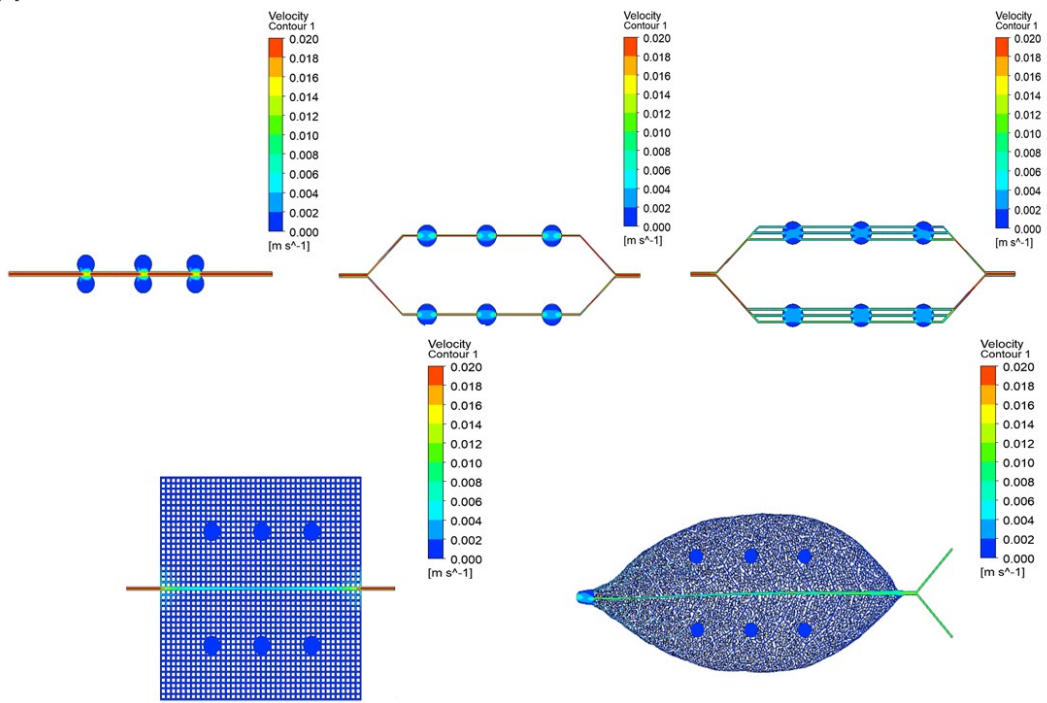
^d. Research Institute for Intelligent Wearable Systems, the Hong Kong Polytechnic University, Hung Hom, Kowloon, Hong Kong SAR, China.

^e. Department of Electrical and Electronic Engineering, The University of Hong Kong, Hong Kong SAR, China.

* Corresponding author.

E-mail address: yuhe.yang@polyu.edu.hk (Y. Yang), xin.zhao@polyu.edu.hk (X. Zhao).

A



B

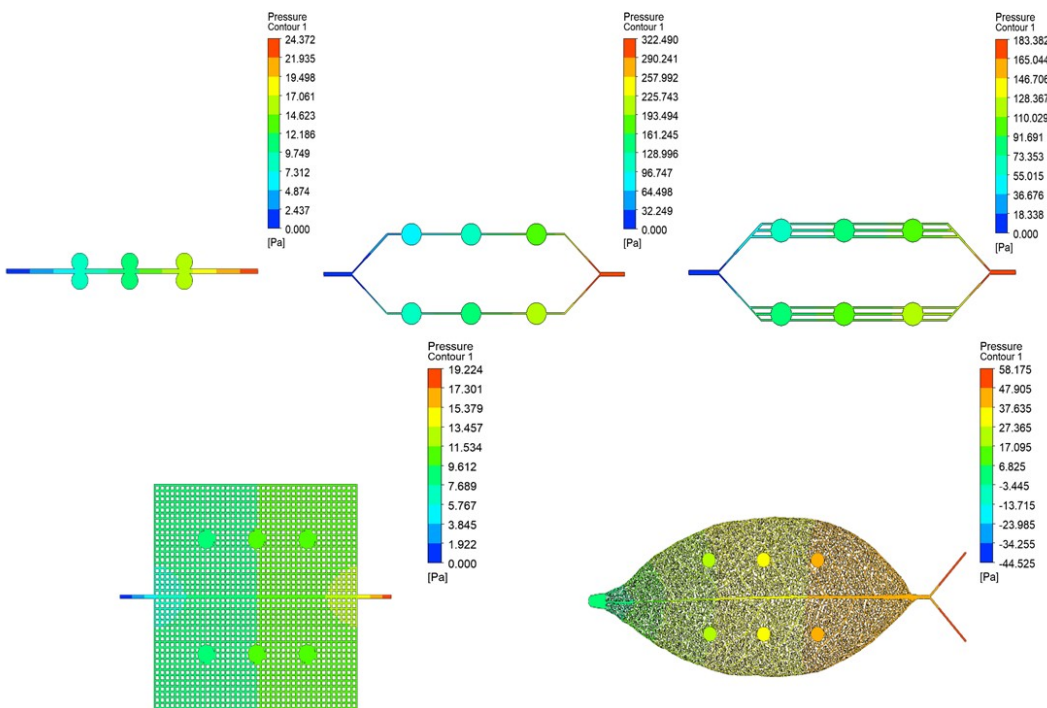


Fig. S1 A) Velocity distribution and B) pressure distribution of the leaf vein chip and other microfluidic chips with chambers and different degrees of branching.

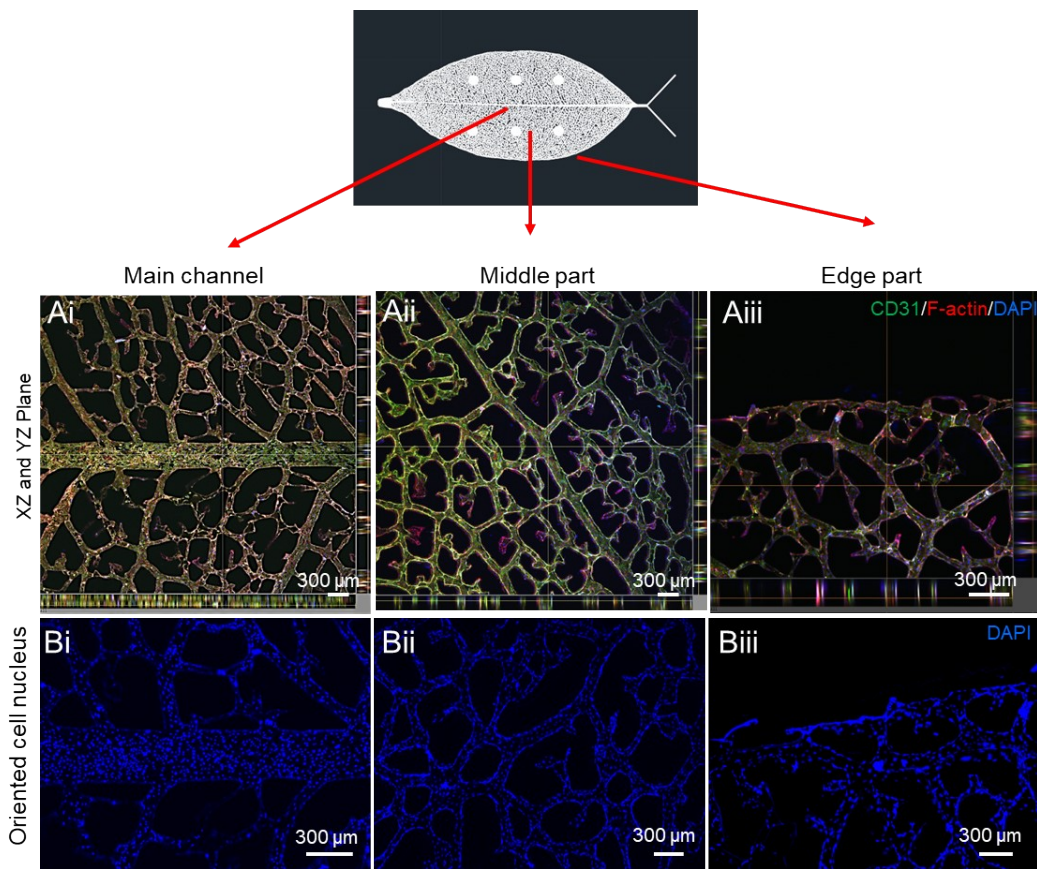


Fig. S2 A) The cross-sectional view of CD31/F-actin/DAPI staining of the (i) main channel, (ii) middle part and (iii) edge part. B) Oriented cell nucleus along the (i) main channel, (ii) middle part and (iii) edge part.

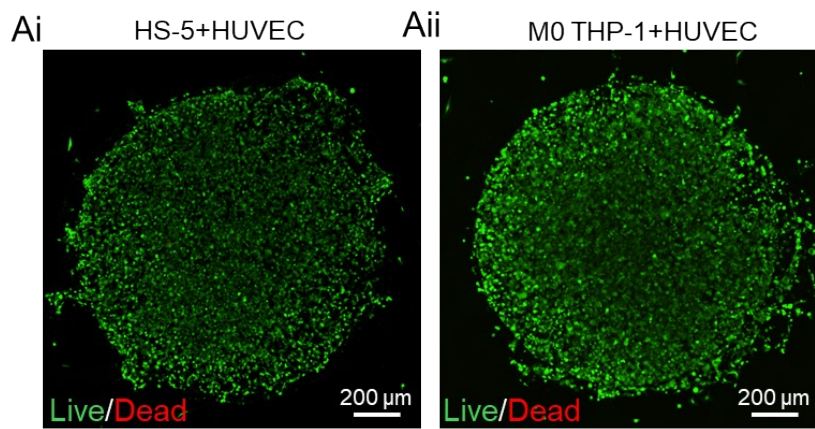


Fig. S3 A) Live/dead staining of (i) HS-5 and HUVEC cell-loaded hydrogel and (ii) M0 THP-1 and HUVEC cell-loaded hydrogel.

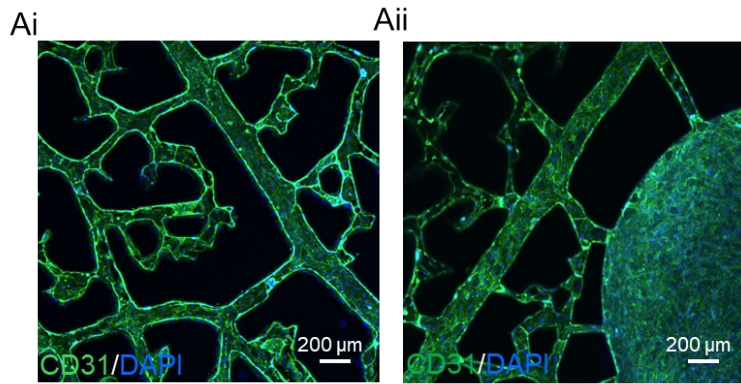


Fig. S4 A) Immunofluorescence images of vascular network in channels (i) and between the chamber and channels (ii) stained with CD31 (green) and DAPI (blue).

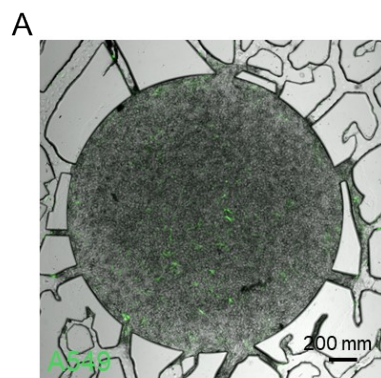


Fig. S5 A) Representative image of A549 cells perfused into the vascular network within the chamber.

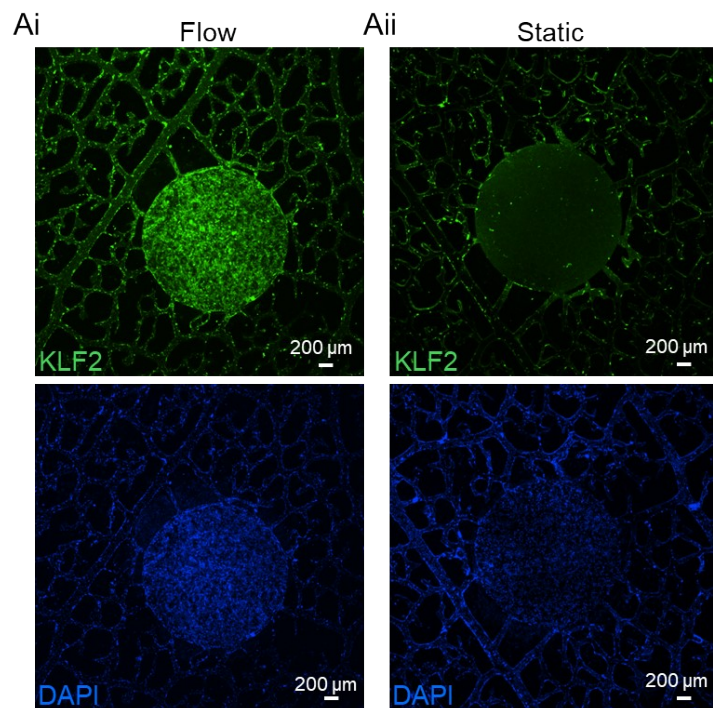


Fig. S6 A) Immunofluorescence images of the leaf vein chip cultured under flow (i) and static (ii) conditions stained with shear-responsive marker KLF2 (green) and DAPI (blue).

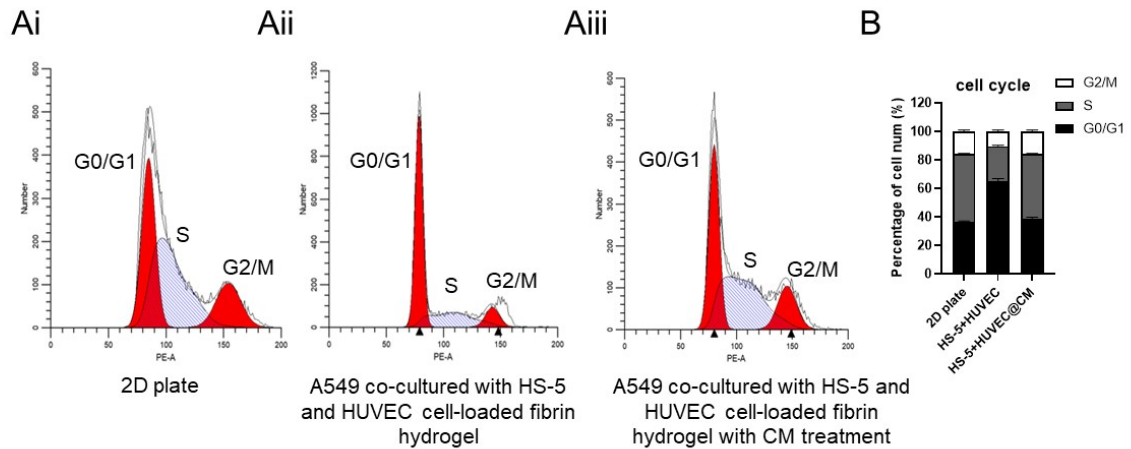
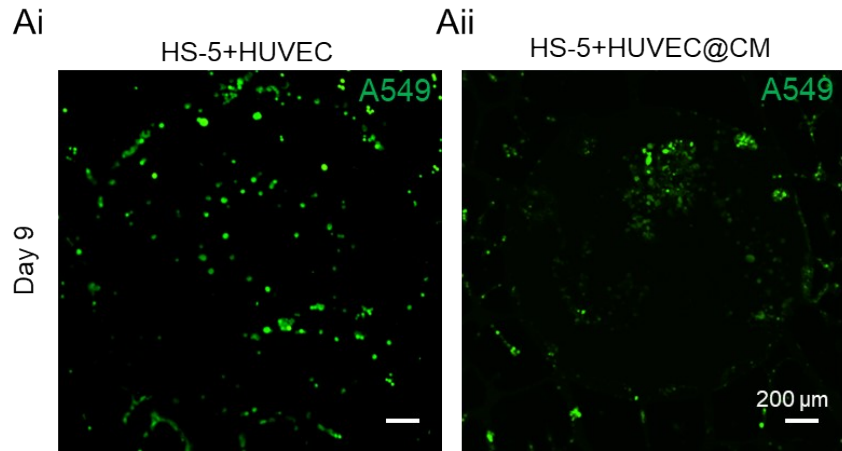


Fig. S7 A) Off-chip cell cycle experiment of (i) A549 cultured in 2D plate, (ii) A549 co-cultured with HS-5 and HUVEC cell-loaded fibrin hydrogel in the transwell system and (iii) A549 co-cultured with HS-5 and HUVEC cell-loaded fibrin hydrogel with tumor conditioned medium (CM) treatment in the transwell system. B) Quantitative cell cycle analysis of tumor cells in three different groups.



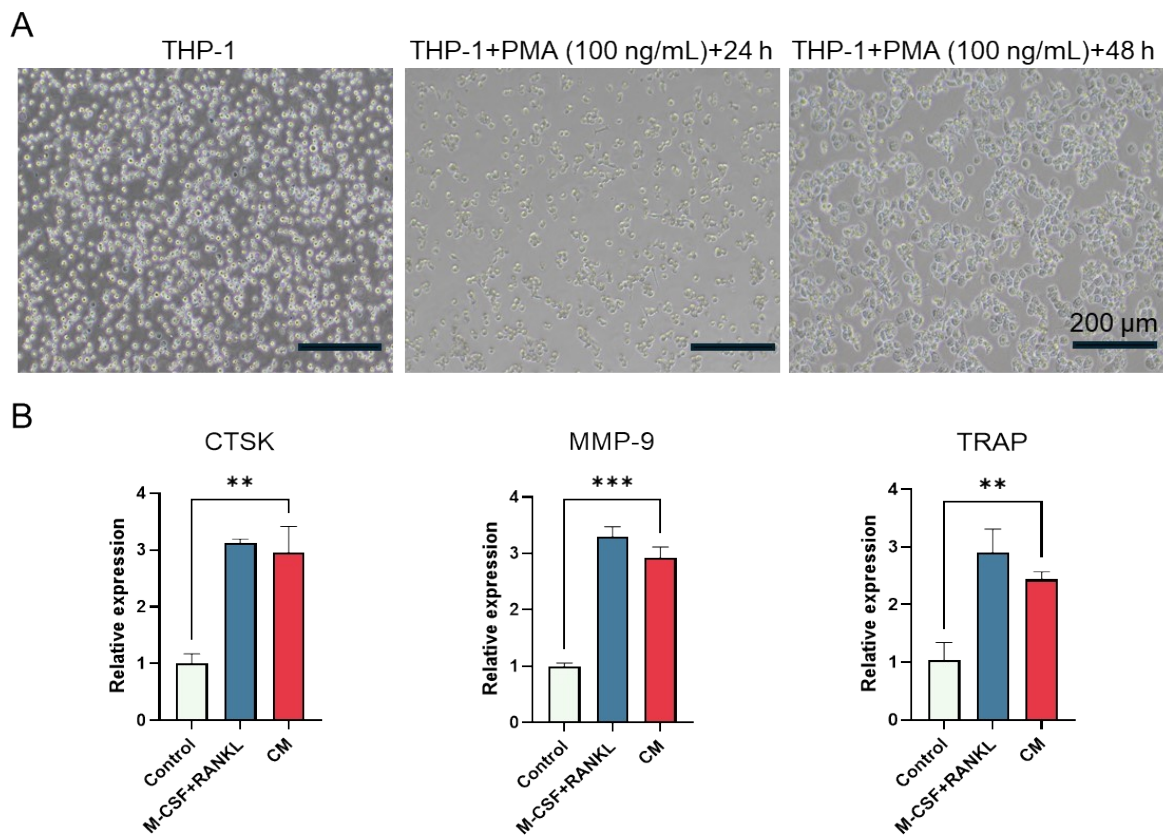


Fig. S9 A) Cell morphology of THP-1 and M0 THP-1 induced by PMA. B) RT-qPCR results of osteoclast gene (CTSK, MMP-9 and TRAP) expression of M0 THP-1 cells induced by M-CSF and RANKL or CM for 5 days. The differences are statistically significant when p values are below 0.05 (*), 0.01 (**), and 0.001 (***)�.

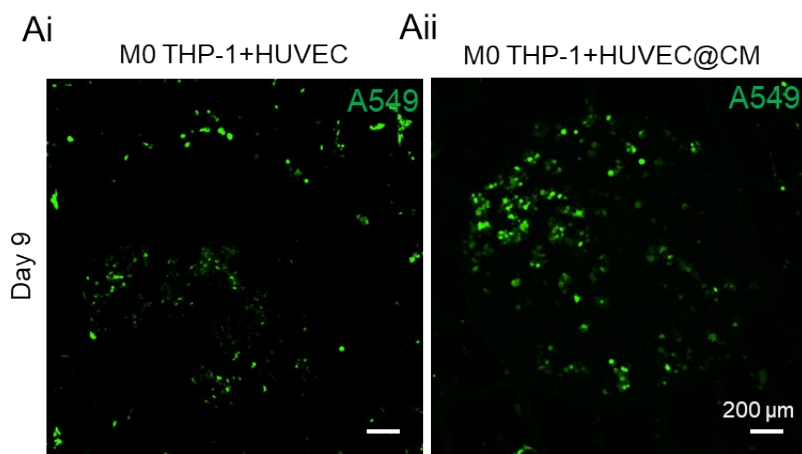


Fig. S10 A) Cell morphology for A549 in vascularized bone environment consisting of M0 THP-1 and HUVEC cells perfused with (i) normal medium (ECM:DMEM=1:1) and (ii) experimental medium (ECM:CM=1:1) on day 9.

Table S1. Average velocity and coefficient of variation (CV) of velocity distribution in the chamber of microfluidic chips from PIV results and pressure drop of microfluidic chips from 2D simulation models.

	No branch	Single branch	Three branches	Grid	Leaf vein
Average velocity (mm/s)	0.29	0.33	0.25	0.04	0.08
Velocity CV (%)	41.30%	30.39%	21.06%	29.91%	27.38%
Pressure drop (Pa)	23.96	322.13	183.03	18.87	116.02

Table S2. Primer sequences in the RT-qPCR.

Genes	Sequences
CTSK	F:5'- AAATCAGGGTCAGTGTGGTCC-3' R:5'-TCATTCTCAGACACACAATCCACTA -3'
MMP-9	F:5'-GCACGACGTCTTCCAGTACC -3' R:5'- GGTTCAACTCACTCCGGGAA-3'
TRAP	F:5'-AAGATGAGAATGGCGTGGGCTA-3' R:5'-ACCCAGTGAGTCTTCAGTCCCAT-3'
BMP-1	F:5'- GCCACGTTCCATCGTTCG-3' R:5'-AGAATGTGTTCCGAGCGTAATG-3'
Wnt-5a	F:5'- GCCAGTATCAATTCCGACATCG-3' R:5'-TCACCGCGTATGTGAAGGC-3'
MIP-3 α	F:5'-GGGTACTAACACTGAGCAGA-3' R:5'-AGTCAAAGTTGCTTGCTTCTGA-3'
TGF- β 2	F:5'-CCATCCCGCCCACTTCTAC-3' R:5'-AGCTCAATCCGTTGTTCAGGC-3'
VCAM-1	F:5'-GGGAAGATGGTCGTGATCCTT-3' R:5'-TCTGGGTTGGTCTCGATTAA-3'
CCL5	F:5'-CCAGCAGTCGTCTTGTAC-3' R:5'-CTCTGGGTTGGCACACACTT-3'